MISSING INTENSITY RESTORATION VIA PERCEPTUALLY OPTIMIZED SUBSPACE PROJECTION BASED ON ENTROPY COMPONENT ANALYSIS

Takahiro Ogawa and Miki Haseyama

Graduate School of Information Science and Technology, Hokkaido University
N-14, W-9, Kita-ku, Sapporo, Hokkaido, 060-0814, Japan
E-mail: ogawa@lmd.ist.hokudai.ac.jp, miki@ist.hokudai.ac.jp

ABSTRACT

A missing intensity restoration method via perceptually optimized subspace projection based on entropy component analysis (ECA) is presented in this paper. The proposed method calculates the optimal subspace of known patches within a target image based on structural similarity (SSIM) index, and the optimal bases are determined based on ECA. Then missing intensity estimation whose results maximize the SSIM index is realized by using a projection onto convex sets (POCS) algorithm whose constraints are the obtained subspace and known intensities within the target image. In this approach, a non-convex maximization problem for calculating the projection onto the subspace is reformulated as a quasi-convex problem, and the restoration of the missing intensities becomes feasible. Experimental results show that our restoration method outperforms previously reported methods.

Index Terms— Missing intensity restoration, image quality assessment, entropy component analysis, POCS algorithm.

1. INTRODUCTION

Many researchers have proposed missing intensity restoration methods since this study affords a number of fundamental applications [1]–[15]. A pioneering work of missing intensity restoration was proposed by Efros et al [4]. Furthermore, in recent years, Drori et al. and Criminisi et al. have developed a fragment-based restoration method [5] and an exemplar-based method [6, 7], respectively, and their methods became benchmarking methods in this field. From a characteristic that the restoration of missing intensities is one of inverse problems, several methods using low-dimensional subspaces for deriving inverse projection to estimate missing intensities have been proposed. For example, Amano et al. proposed an effective PCA-based method that estimates missing textures by back projection for lost pixels [9]. Furthermore, by introducing the kernel methods into PCA [16, 17], its improvement can be also realized [10, 11]. Recently, sparse representation-based image restoration has intensively been studied [12]–[15], [18, 19]. Mairal et al. proposed a representative work based on the sparse-representation [12], and Xu et al. also proposed an improved exemplar-based method by using the sparse representation [15].

In most existing works using low-dimensional subspaces, missing intensities are restored by projection onto these subspaces generated based on minimization of mean square error (MSE). Although the MSE is the most popular metric used as a quality measure, it has been reported that MSE cannot reflect perceptual qualities [20, 21]. Recently, there have been proposed many image quality assessment algorithms [22]–[26]. Among them, the structural similarity (SSIM) index [26] is well known as a representative measure, and it is reported that the SSIM index is superior to the MSE and its variants for several image processing applications [27, 28]. Therefore, by using the SSIM index, successful restoration using perceptually optimized subspaces can be expected.

In this paper, we present a new missing intensity restoration method via perceptually optimized subspace projection based on entropy component analysis (ECA). The proposed method performs the generation of the subspace optimized in terms of the SSIM index for estimating missing intensities within a target image. In this approach, ECA-based optimal orthonormal basis selection is adopted since it is reported in [29] that the bases selected by ECA is superior to PCA-based bases in several tasks. Then the proposed method enables the missing intensity restoration by using a projection onto convex sets (POCS) algorithm [30] whose constraints are the obtained subspace and known intensities within the target image. Note that in this approach, a non-convex problem for calculating the projection onto the subspace is reformulated as a quasi-convex problem. Consequently, we can derive the optimal solution based on the SSIM index, and successful missing intensity restoration is expected.

2. SSIM INDEX

The SSIM index is proposed as a similarity between two vectors $\mathbf{x}_1$ and $\mathbf{x}_2$ ($\in \mathbf{R}^n$), and its simplified definition is shown as follows:

$$\mathrm{SSIM}(\mathbf{x}_1, \mathbf{x}_2) = \frac{\left(2\mu_{\mathbf{x}_1}\mu_{\mathbf{x}_2} + C_1\right)\left(2\sigma_{\mathbf{x}_1,\mathbf{x}_2} + C_2\right)}{\left(\mu^2_{\mathbf{x}_1} + \mu^2_{\mathbf{x}_2} + C_1\right)\left(\sigma^2_{\mathbf{x}_1} + \sigma^2_{\mathbf{x}_2} + C_2\right)},$$

where $\mu_{\mathbf{x}_i}$ and $\sigma^2_{\mathbf{x}_i}$ ($i = 1, 2$) are respectively the mean and the variance of $\mathbf{x}_i$. Furthermore, $\sigma_{\mathbf{x}_1,\mathbf{x}_2}$ is the cross covariance between $\mathbf{x}_1$ and $\mathbf{x}_2$. The constants C_1 and C_2 are necessary for avoiding instability when the denominators are very close to zero. The SSIM index is defined by separately calculating three similarities in terms of luminance, variance and structure, which are derived on the basis of the human visual system (HVS) not accounted for by MSE. Therefore, perceptually optimized restoration can be expected by using this quality measure.

3. MISSING INTENSITY RESTORATION VIA SSIM-BASED ECA SUBSPACE PROJECTION

The missing intensity restoration method via SSIM-based ECA subspace projection is presented in this section. In the proposed method,

This work was partly supported by Grant-in-Aid for Scientific Research (B) 25280036 and Grant-in-Aid for Young Scientists (B) 22700088, Japan Society for the Promotion of Science (JSPS).

978-1-4799-2893-4/14/$31.00 ©2014 IEEE

we clip a patch f ($w \times h(= N)$ pixels) including missing areas Ω. From known areas $\bar{\Omega}$ within the target patch f, we try to restore the intensities of its missing areas Ω by using the subspace obtained from the other known parts within the target image. For the following explanation, we define two vectors, whose elements are respectively intensities within f and $\bar{\Omega}$, as $\mathbf{x}(\in \mathbf{R}^N)$ and $\mathbf{y}(\in \mathbf{R}^{N_{\bar{\Omega}}})$, where $N_{\bar{\Omega}}$ is the number of pixels within the areas $\bar{\Omega}$.

First, the proposed method performs the estimation of the ECA subspace optimized in terms of the SSIM index (See **3.1**). Furthermore, we perform the missing intensity restoration using the POCS algorithm whose constraints are the obtained subspace and the known intensities within $\bar{\Omega}$ (See **3.2**).

3.1. SSIM-Based ECA Subspace Estimation Algorithm

In order to obtain samples for generating the subspace, we clip known patches f_i ($i = 1, 2, \cdots, L$) whose size is the same as that of f from the target image in the same interval. Then, for each patch f_i, we define a vector $\mathbf{x}_i$ ($\in \mathbf{R}^N$), which corresponds to $\mathbf{x}$. First, from $\mathbf{x}_i$ ($i = 1, 2, \cdots, L$), we calculate M orthonormal bases which span the subspace optimized in terms of the SSIM index, where M is smaller than N. In this approach, it is difficult to simultaneously obtain all bases optimized with the SSIM index. Therefore, we adopt the simplest algorithm that selects the optimal bases one by one, and it is similar to several matching pursuit algorithms [31, 32, 33]. The details of mth ($m = 1, 2, \cdots, M$) optimal basis calculation are shown below.

In mth iteration, i.e., mth optimal basis calculation, we first define the following vector approximating $\mathbf{x}_i$ ($i = 1, 2, \cdots, L$):

$$\mathbf{x}_i^{(m)} = \begin{bmatrix} \hat{\mathbf{U}}^{(m-1)} & \mathbf{u}^{(m)} \end{bmatrix} \begin{bmatrix} \mathbf{a}_i^{(m-1)} \\ a_i^{(m)} \end{bmatrix},$$

where $\hat{\mathbf{U}}^{(m-1)} = [\hat{\mathbf{u}}^{(1)}, \hat{\mathbf{u}}^{(2)}, \cdots, \hat{\mathbf{u}}^{(m-1)}]$ is a fixed $N \times (m-1)$ matrix which contains $m-1$ bases previously calculated in $m-1$ iterations. We estimate the optimal orthonormal basis $\hat{\mathbf{u}}^{(m)}$ of $\mathbf{u}^{(m)}$ which provides the best representation performance for all known patches f_i ($i = 1, 2, \cdots, L$) based on the SSIM index. Specifically, it can be calculated by solving the following problem:

$$\begin{aligned} \left\{\hat{\mathbf{u}}^{(m)}, \hat{\mathbf{a}}^{(m)}\right\} &= \arg\max_{\mathbf{u}^{(m)}, \mathbf{a}^{(m)}} \sum_{i=1}^{L} \mathrm{SSIM}(\mathbf{x}_i, \mathbf{x}_i^{(m)}) \\ &\quad \text{subject to} \quad \|\mathbf{u}^{(m)}\|^2 = 1 \\ &\quad \mathbf{u}^{(m)\prime}\mathbf{u}^{(l)} = 0 \quad (l = 1, 2, \cdots, m-1), \end{aligned} \tag{1}$$

where $\mathbf{a}^{(m)}$ is a set of $\mathbf{a}_1^{(m)}, \mathbf{a}_2^{(m)}, \cdots, \mathbf{a}_L^{(m)}$, and $\mathbf{a}_i^{(m)} = [\mathbf{a}_i^{(m-1)\prime}, a_i^{(m)}]'$ ($i = 1, 2, \cdots, L$). Furthermore, vector/matrix transpose is denoted by the superscript $'$. The optimal basis $\hat{\mathbf{u}}^{(m)}$ and the optimal coefficient vectors $\hat{\mathbf{a}}_i^{(m)}$ ($i = 1, 2, \cdots, L$) are calculated by applying the constrained steepest ascend algorithm to Eq. (1). The steepest ascend algorithm does not necessarily provide the global optimal solution in Eq. (1), but this algorithm can save the computation cost compared to the algorithm shown in the following subsection. From this reason, we utilize this scheme in the proposed method. By iterating the above procedures M times, we can obtain the optimal M orthonormal bases $\hat{\mathbf{u}}^{(m)}$ ($m = 1, 2, \cdots, M$) based on the SSIM index.

From the obtained M orthonormal bases $\hat{\mathbf{u}}^{(m)}$ ($m = 1, 2, \cdots, M$), we further select D bases $\hat{\mathbf{u}}_d$ ($d = 1, 2, \cdots, D$) by using the algorithm in ECA [29]. Specifically, D bases, whose values $\sum_{i=1}^{L} \left(\hat{\mathbf{u}}^{(m)\prime}\mathbf{x}_i\right)^2$ based on Renyi quadratic entropy are larger than those of the other bases, are selected as the optimal bases $\hat{\mathbf{u}}_d$ ($d = 1, 2, \cdots, D$). ECA can select the optimal bases in such a way that they can successfully represent cluster structures of the target samples. Since the target image contains several kinds of textures, i.e., the samples $\mathbf{x}_i$ ($i = 1, 2, \cdots, L$) have cluster structures, we introduce ECA into the selection of the optimal orthonormal bases. Finally, we obtain the matrix $\hat{\mathbf{U}} = [\hat{\mathbf{u}}_1, \hat{\mathbf{u}}_2, \cdots, \hat{\mathbf{u}}_D]$ including these selected bases, i.e., the optimal subspace.

3.2. Missing Intensity Restoration Algorithm

For restoring the missing areas Ω within the target patch f, the proposed method uses the POCS algorithm [30] whose constraints are shown below.

[Constraint 1]

Since the intensities of the vector $\mathbf{y}$ within $\bar{\Omega}$ are all known, their values are fixed in the vector $\mathbf{x}$, i.e., $\mathbf{y} = \mathbf{E}\mathbf{x}$ is satisfied, where $\mathbf{E}$ is a matrix extracting only the known intensities in $\bar{\Omega}$.

[Constraint 2]

The vector $\mathbf{x}$ of the target patch f is in the subspace spanned by the orthonormal bases $\hat{\mathbf{u}}_d$ ($d = 1, 2, \cdots, D$).

The proposed method performs the projection onto these two constraints iteratively to obtain the final estimation result $\hat{\mathbf{x}}$ of the unknown vector $\mathbf{x}$. Note that for each iteration t, we have to calculate the SSIM-based projection onto the subspace spanned by the bases $\hat{\mathbf{u}}_d$ ($d = 1, 2, \cdots, D$). Specifically, in tth iteration, we have to estimate the optimal linear combination

$$\hat{\mathbf{x}}^{(t)} = \hat{\mathbf{U}}\hat{\mathbf{a}}^{(t)} \tag{2}$$

approximating the target vector $\mathbf{x}^{(t)}$ which satisfies Constraint 1, where

$$\hat{\mathbf{a}}^{(t)} = \arg\max_{\mathbf{a}^{(t)}} \mathrm{SSIM}\left(\mathbf{x}^{(t)}, \hat{\mathbf{U}}\mathbf{a}^{(t)}\right). \tag{3}$$

In the above equation,

$$\begin{aligned} \mathrm{SSIM}\left(\mathbf{x}^{(t)}, \hat{\mathbf{U}}\mathbf{a}^{(t)}\right) &= \left[\frac{2\mu_{\mathbf{x}^{(t)}}\mu_{\hat{\mathbf{U}}\mathbf{a}^{(t)}} + C_1}{\mu_{\mathbf{x}^{(t)}}^2 + \mu_{\hat{\mathbf{U}}\mathbf{a}^{(t)}}^2 + C_1}\right]\left[\frac{2\sigma_{\mathbf{x}^{(t)},\hat{\mathbf{U}}\mathbf{a}^{(t)}} + C_2}{\sigma_{\mathbf{x}^{(t)}}^2 + \sigma_{\hat{\mathbf{U}}\mathbf{a}^{(t)}}^2 + C_2}\right] \\ &= \left[\frac{2\left(\frac{1}{N}\mathbf{1}'\mathbf{x}^{(t)}\right)\left(\boldsymbol{\mu}_{\hat{\mathbf{U}}}'\mathbf{a}^{(t)}\right) + C_1}{\left(\frac{1}{N}\mathbf{1}'\mathbf{x}^{(t)}\right)^2 + \left(\boldsymbol{\mu}_{\hat{\mathbf{U}}}'\mathbf{a}^{(t)}\right)^2 + C_1}\right] \\ &\quad \times \left[\frac{2\mathbf{x}^{(t)\prime}\mathbf{H}\hat{\mathbf{U}}\mathbf{a}^{(t)} + NC_2}{\mathbf{x}^{(t)\prime}\mathbf{H}\mathbf{x}^{(t)} + \mathbf{a}^{(t)\prime}\hat{\mathbf{U}}'\mathbf{H}\hat{\mathbf{U}}\mathbf{a}^{(t)} + NC_2}\right], \end{aligned} \tag{4}$$

and $\boldsymbol{\mu}_{\hat{\mathbf{U}}} = \frac{1}{N}\hat{\mathbf{U}}'\mathbf{1}$, where $\mathbf{1} = [1, 1, \cdots, 1]'$ is an $N \times 1$ vector. Furthermore, $\mathbf{H} = \mathbf{I} - \frac{1}{N}\mathbf{1}\mathbf{1}'$ is an $N \times N$ centering matrix, where $\mathbf{I}$ is the identity matrix.

Since Eq. (4) is a nonconvex function of $\mathbf{a}^{(t)}$, we introduce the calculation scheme shown in [27] for converting it into a quasi-convex problem. First, we note the first term in Eq. (4) is a function only of $\boldsymbol{\mu}_{\hat{\mathbf{U}}}'\mathbf{a}^{(t)} \left(= \rho^{(t)}\right)$. Thus, the problem in Eq. (3) is rewritten as follows:

$$\begin{aligned} &\max_{\mathbf{a}^{(t)}} \left(\frac{2\mathbf{x}^{(t)\prime}\mathbf{H}\hat{\mathbf{U}}\mathbf{a}^{(t)} + NC_2}{\mathbf{x}^{(t)\prime}\mathbf{H}\mathbf{x}^{(t)} + \mathbf{a}^{(t)\prime}\hat{\mathbf{U}}'\mathbf{H}\hat{\mathbf{U}}\mathbf{a}^{(t)} + NC_2}\right) \\ &\qquad \text{subject to } \boldsymbol{\mu}_{\hat{\mathbf{U}}}'\mathbf{a}^{(t)} = \rho^{(t)}. \end{aligned} \tag{5}$$

Therefore, the overall problem is reformulated to find the highest SSIM index in Eq. (3) by searching over range of $\rho^{(t)}$. Furthermore, Eq. (5) is converted into a quasi-convex optimization problem as

$$\begin{aligned} &\min : \tau \\ &\text{subject to} \left[\begin{array}{c} \max : \left(\frac{2\mathbf{x}^{(t)\prime}\mathbf{H}\hat{\mathbf{U}}\mathbf{a}^{(t)} + NC_2}{\mathbf{x}^{(t)\prime}\mathbf{H}\mathbf{x}^{(t)} + \mathbf{a}^{(t)\prime}\hat{\mathbf{U}}'\mathbf{H}\hat{\mathbf{U}}\mathbf{a}^{(t)} + NC_2}\right) \le \tau \\ \text{subject to} \quad \boldsymbol{\mu}_{\hat{\mathbf{U}}}'\mathbf{a}^{(t)} = \rho^{(t)} \end{array}\right] \end{aligned} \tag{6}$$

Table 1. Performance comparison (SSIM index) between the previously reported methods and our method.

Test image	Reference [7]	Reference [8]	Reference [15]	Reference [9]	Reference [10]	Reference [11]	Our method
Image 1	0.7336	0.7282	0.7583	0.6311	0.6146	0.7249	**0.7871**
Image 2	0.7369	0.7446	0.7439	0.6657	0.6832	0.7305	**0.7476**
Image 3	0.6617	0.6695	0.6983	0.5822	0.5796	0.6735	**0.7378**
Image 4	0.7159	0.7066	0.7293	0.7158	0.7100	0.7529	**0.7843**
Image 5	0.7059	0.6954	0.7155	0.6050	0.6388	0.7287	**0.7436**
Image 6	0.6962	0.6827	0.7086	0.6269	0.6484	0.7363	**0.7440**
Average	0.7084	0.7045	0.7257	0.6378	0.6458	0.7245	**0.7574**

since minimization of τ is the same as finding the least upper bound of Eq. (5). Furthermore, Eq. (6) is rewritten as

$$\begin{aligned}&\min: \tau\\ &\text{subject to}\\ &\begin{bmatrix}\min: \left[\tau\left(\mathbf{x}^{(t)\prime}\mathbf{H}\mathbf{x}^{(t)} + \mathbf{a}^{(t)\prime}\mathbf{K}_1\mathbf{a}^{(t)} + NC_2\right) - \left(\mathbf{x}^{(t)\prime}\mathbf{K}_2\mathbf{a}^{(t)} + NC_2\right)\right] \geq 0\\ \text{subject to} \quad \boldsymbol{\mu}_{\hat{\mathbf{U}}}{}'\mathbf{a}^{(t)} = \rho^{(t)}\end{bmatrix}\end{aligned}$$

since the denominator in Eq. (5) is strictly positive, allowing us to multiply through and rearrange terms. Note that

$$\mathbf{K}_1 = \hat{\mathbf{U}}'\mathbf{H}\hat{\mathbf{U}},$$

and

$$\mathbf{K}_2 = 2\mathbf{H}\hat{\mathbf{U}}.$$

Then, in the proposed method, τ becomes a true upper bound if

$$\begin{bmatrix}\max_{\mathbf{a}^{(t)}} \tau\left(\mathbf{x}^{(t)\prime}\mathbf{H}\mathbf{x}^{(t)} + \mathbf{a}^{(t)\prime}\mathbf{K}_1\mathbf{a}^{(t)} + NC_2\right) - \left(\mathbf{x}^{(t)\prime}\mathbf{K}_2\mathbf{a}^{(t)} + NC_2\right) \geq 0\\ \text{subject to} \quad \boldsymbol{\mu}_{\hat{\mathbf{U}}}{}'\mathbf{a}^{(t)} = \rho^{(t)}\end{bmatrix}$$

has a non-negative value. The proposed method adopts the Lagrange multiplier approach shown as follows:

$$\begin{aligned}\mathcal{L} \;=\;& \tau\left(\mathbf{x}^{(t)\prime}\mathbf{H}\mathbf{x}^{(t)} + \mathbf{a}^{(t)\prime}\mathbf{K}_1\mathbf{a}^{(t)} + NC_2\right) - \left(\mathbf{x}^{(t)\prime}\mathbf{K}_2\mathbf{a}^{(t)} + NC_2\right)\\ &+\lambda\left(\boldsymbol{\mu}_{\hat{\mathbf{U}}}{}'\mathbf{a}^{(t)} - \rho^{(t)}\right).\end{aligned}$$

Then, by solving the above problem, we can obtain the optimal vector $\hat{\mathbf{a}}^{(t)}$ which provides the approximation vector $\hat{\mathbf{x}}^{(t)}$ in Eq. (2). Note that τ can be obtained by using the standard bisection procedures. From the result $\hat{\mathbf{x}}$ obtained through the POCS algorithm, the proposed method outputs the estimated intensities in the missing areas Ω.

As shown in the above procedures, we can restore the missing areas Ω within the target patch f. The proposed method clips patches including missing areas and performs their restoration to estimate all missing intensities. Specifically, we search patches including missing pixels based on the patch priority in [7], and their missing areas are restored. Then the restoration of the target image can be completed.

4. EXPERIMENTAL RESULTS

In this section, we show experimental results for verifying the performance of the proposed method. In this experiment, we prepared six kinds of test images shown in Fig. 1 and added missing regions to these images. We assumed that positions of the missing pixels were known in this experiment. For the corrupted images, we performed the restoration of the missing areas by using the proposed method and the previously reported methods [7, 8, 15, 9, 10, 11]. The method in [7] is a representative exemplar-based method using the selection of the best patches which enable MSE-based optimal approximation. The improved versions of [7] have been proposed in [8, 15], where the method in [15] tries to perform the improvement by using the sparse representation which is also based on MSE. Therefore, in this experiment, we adopted these methods [7, 8, 15] and regarded the methods in [8, 15] as state-of-the-art methods. Furthermore, since the methods in [9] and [10, 11] respectively utilize the subspaces obtained by PCA and kernel PCA for restoring missing areas, i.e., the subspaces realizing the least-square approximation in the input space and the high-dimensional feature space, they were adopted in this experiment. In addition, since we can regard the method in [11] as the state-of-the-art approach, it is suitable for the comparison of our perceptually optimized method. In this experiment, since the patch size was fixed to 19, the number of training patches f_i becomes smaller. Since this comparison scheme was adopted in several papers, we also used such difficult conditions in order to make the difference in the performance of the proposed method and the previously reported methods clearer.

The results restored by the previously reported methods and the proposed method are respectively shown in the third and forth columns of Fig. 1. In this figure, we only show the result of one previously reported method for each test image due to the limitation of pages. From the obtained results shown in Fig. 1, it can be seen that the proposed method achieves more accurate missing intensity restoration than those of the previously reported methods. Finally, we show results of quantitative evaluation obtained from the previously reported methods and the proposed method. Table 1 shows the results of the SSIM index calculated between the original images and the restored images obtained by those methods. Note that the values shown in this table were calculated from only the restored areas. From this table, we can confirm that the proposed method achieves the improvement since our method is optimized with this criterion. Therefore, the perceptually optimized method is suitable for the missing intensity restoration.

5. CONCLUSIONS

In this paper, a missing intensity restoration method via perceptually optimized subspace projection based on ECA has been presented. Our method performs the calculation of the subspace optimized in terms of the SSIM index based on ECA which can represent cluster structures of the target data. Then the POCS algorithm, whose constraints are the obtained subspace and the known intensities within the target image, is adopted to estimate the missing intensities. In this approach, the projection which maximizes the SSIM index is realized by converting its problem into the quasi-convex problem. Consequently, impressive improvement of the proposed method over the previously reported methods can be confirmed.

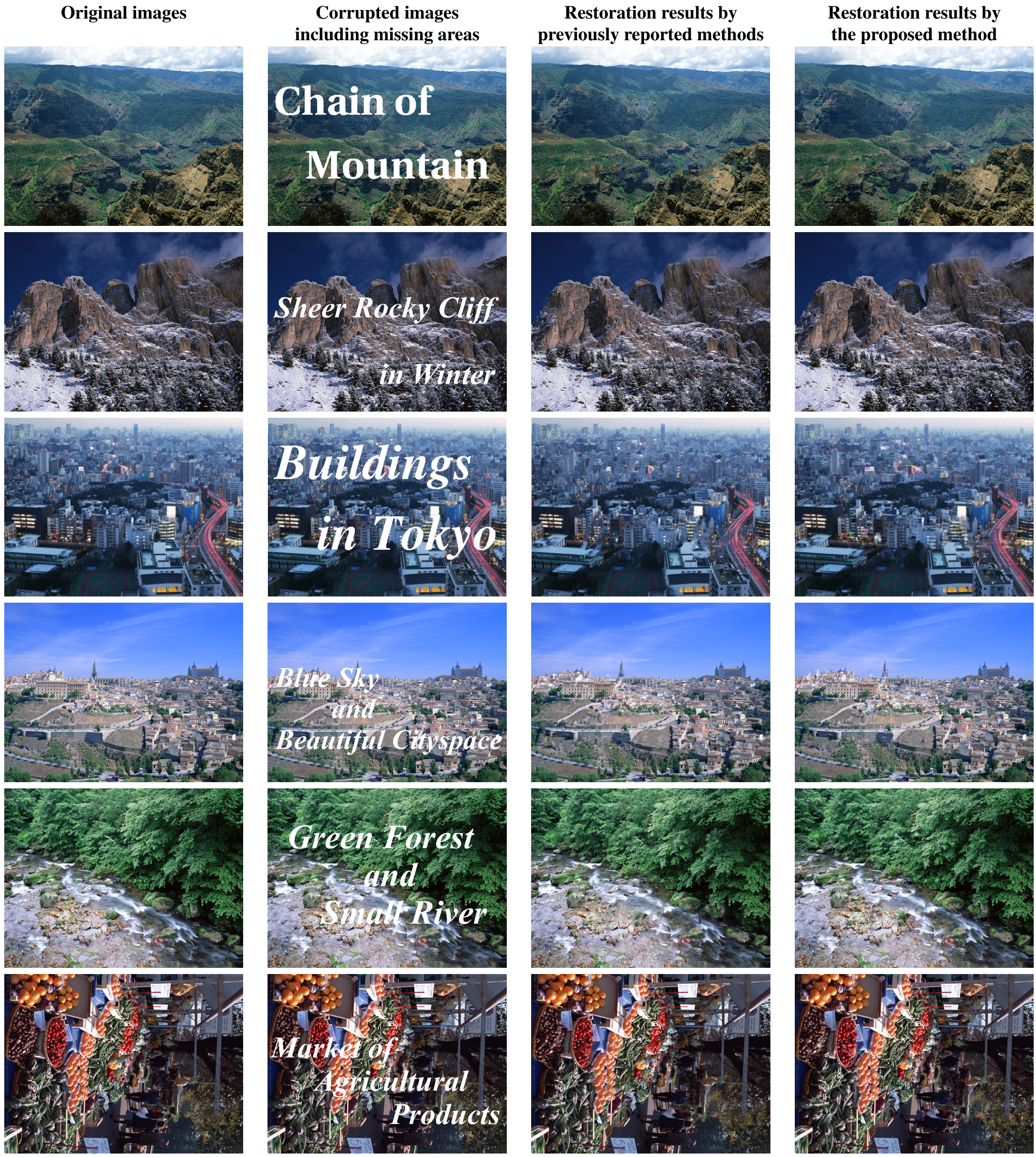

Fig. 1. Restoration results obtained by the previously reported methods and the proposed method. Six test images are used, and they respectively correspond to Images 1–6. Note that the previously reported methods used for restoring Images 1–6 are respectively Ref [7], Ref [8], Ref [15], Ref [9], Ref [10] and Ref [11]. The sizes of Images 1–6 are 480×360 pixels, 640×480 pixels, 480×360 pixels, 640×480 pixels, 640×480 pixels and 640×480 pixels, respectively. The percentages of missing areas are 8.9%, 5.4%, 10.7%, 5.9%, 7.1% and 6.2% in Images 1–6, respectively.

6. REFERENCES

[1] C. Ballester, M. Bertalmio, V. Caselles, G. Sapiro, "Filling-in by joint interpolation of vector fields and gray levels," *IEEE Transactions on Image Processing*, vol.10, no.8, pp.1200–1211, 2001.

[2] A. Kokaram, "A statistical framework for picture reconstruction using 2D AR models," *Image and Vision Computing*, vol.22, no.2, 1, pp.165–171, 2004.

[3] M. Bertalmio, L. Vese, G. Sapiro, and S. Ssher, "Simultaneous structure and texture image inpainting," *IEEE Transactions on Image Processing*, vol. 12, no. 8, pp. 882–889, 2003.

[4] A. A. Efros and T. K. Leung, "Texture synthesis by nonparametric sampling," *IEEE International Conference on Computer Vision,* Corfu, Greece, pp.1033–1038, 1999.

[5] I. Drori, D. Cohen-Or, and H. Teshurun, "Fragment-based image completion," *ACM SIGGRAPH*, pp. 303–312, 2003.

[6] A. Criminisi, P. Perez, and K. Toyama, "Object removal by exemplar-based inpainting," *IEEE Computer Vision and Pattern Recognition*, 2003.

[7] A. Criminisi, P. Perez, and K. Toyama, "Region filling and object removal by exemplar-based image inpainting," *IEEE Transactions on Image Processing*, vol. 13, no. 9, pp. 1200–1212, 2004.

[8] T. H. Kwok, H. Sheung, and C. C. L. Wang, "Fast query for exemplar-based image completion," *IEEE Transactions on Image Processing*, vol. 19, no. 12, pp. 3106–3115, 2010.

[9] T. Amano and Y. Sato, "Image interpolation using BPLP method on the eigenspace," *Systems and Computers in Japan*, vol.38, no.1, pp.87–96, 2007.

[10] K. I. Kim, M. O. Franz , B. Schölkoph, "Iterative kernel principal component analysis for image modeling," *IEEE Transactions on Pattern Analysis and Machine Intelligence*, vol.27, no.9, pp. 1351–1366, 2005.

[11] T. Ogawa, M. Haseyama, "Missing intensity interpolation using a kernel PCA-Based POCS algorithm and its applications," *IEEE Transactions on Image Processing*, vol. 20, no. 2, pp. 417–432, 2011.

[12] J. Mairal, M. Elad, and G. Sapiro, "Sparse representation for color image restoration," *IEEE Transactions on Image Processing*, vol.17, no.1, pp. 53–69, 2008.

[13] B. Wohlberg, "Inpainting with sparse linear combinations of exemplars," *IEEE International Conference on Acoustics, Speech, and Signal Processing*, pp. 689–692, 2009.

[14] B. Shen, W. Hu, Y. Zhang, and Y.-J. Zhang, "Image inpainting via sparse representation," *IEEE International Conference on Acoustics, Speech, and Signal Processing*, pp. 697–700, 2009.

[15] Z. Xu and J. Sun, "Image Inpainting by Patch Propagation Using Patch Sparsity," *IEEE Transactions on Image Processing*, vol. 19, no. 5, pp. 1153–1165, 2010.

[16] B. Schölkopf, S. Mika, C. J. C. Burges, P. Knirsch, K.-R. Müller, G. Rätsch, and A. J. Smola, "Input space versus feature space in kernel-based methods," *IEEE Transactions on Neural Networks*, vol.10, no.5, pp.1000–1017, 1999.

[17] S. Mika, B. Schölkopf, A. Smola, K.-R. Müller, M. Scholz, and G. Rätsch, "Kernel PCA and de-noising in feature spaces," *Advances in Neural Information Processing Systems*, vol.11, pp.536–542, 1999.

[18] M. Aharon, M. Elad, A. Bruckstein, "K-SVD: An algorithm for designing overcomplete dictionaries for sparse representation," *IEEE Transactions on Signal Processing*, vol.54, no.11, pp. 4311–4322, 2006.

[19] M. Elad and M. Aharon, "Image denoising via sparse and redundant representations over learned dictionaries," *IEEE Transactions on Image Processing*, vol. 15, no. 12, pp. 3736–3745, 2006.

[20] B. Girod, "What's wrong with mean-squared error?," *Digital Images and Human Vision*, A.B. Watson, Ed. Cambridge, MA: MIT Press, pp.207–220, 1993.

[21] Z. Wang and A. C. Bovik, "Modern image quality assessment," *Morgan & Claypool Publishers*, Mar. 2006.

[22] N. Damera-Venkata, T. D. Kite, W. S. Geisler, B. L. Evans, and A. C. Bovik, "Image quality assessment based on a degradation model," *IEEE Transactions on Image Processing*, vol. 4, no. 4, pp.636–650, 2000.

[23] H. R. Sheikh, A. C. Bovik, and G. de Veciana, "An information fidelity criterion for image quality assessment using natural scene statistics," *IEEE Transactions on Image Processing*, vol. 14, no. 12, pp.2117–2128, 2005.

[24] H. R. Sheikh and A. C. Bovik, "Image information and visual quality," *IEEE Transactions on Image Processing*, vol. 15, no. 2, pp.430–444, 2006.

[25] H. R. Sheikh, M. F. Sabir, and A. C. Bovik, "A statistical evaluation of recent full reference image quality assessment algorithms," *IEEE Transactions on Image Processing*, vol. 15, no. 11, pp. 3440–3451, 2006.

[26] Z. Wang, A. C. Bovik, H. R. Sheikh, and E. P. Simoncelli, "Image quality assessment: From error visibility to structural similarity," *IEEE Transactions on Image Processing*, vol. 13, no. 4, pp. 600–612, 2004.

[27] S. S. Channappayya, A. C. Bovik, and C. Caramanis, R. W. Heath, "Design of linear equalizers optimized for the structural similarity index," *IEEE Transactions on Image Processing*, vol. 17, no. 6, pp. 857–872, Jun. 2008.

[28] A. Rehman, M. Rostami, Z. Wang, D. Brunet, and E. R. Vrscay, "SSIM-inspired image restoration using sparse representation," *EURASIP Journal on Advances in Signal Processing*, 2012:16, 2012.

[29] R. Jenssen, "Kernel Entropy Component Analysis," *IEEE Transactions on Pattern Analysis and Machine Intelligence*, vol. 32, no. 5, pp. 847–860, 2010.

[30] D. C. Youla and H. Webb, "Image restoration by the method of convex projections: Part 1 – Theory," *IEEE Transactions on Medical Imaging,* vol.MI-1, pp.81–94, Oct. 1982.

[31] S. Mallat and Z. Zhang, "Matching pursuits with time-frequency dictionaries," *IEEE Transactions on Signal Processing*, vol. 41, no. 12, pp.3397–3415, 1993.

[32] S. Chen, S. A. Billings, and W. Luo, "Orthogonal least squares methods and their applications to non-linear system identification," *Int. J. Contr.*, vol. 50, no. 5, pp. 1873–1896, 1989.

[33] J. A. Tropp, "Greed is good: Algorithmic results for sparse approximation," *IEEE Transactions on Information Theory*, vol. 50, no. 10, pp. 2231–2242, 2004.